Stochastic observer design for robot impact detection based on inverse dynamic model under uncertainties

Nolwenn Briquet-Kerestedjian, Maria Makarov, Mathieu Grossard, Pedro Rodriguez-Ayerbe

Stochastic observer design for robot impact detection based on inverse dynamic model under uncertainties[1]

N. Briquet-Kerestedjian [*,**] **M. Makarov** [*] **M. Grossard** [**]
P. Rodriguez-Ayerbe [*]

[*] *Laboratoire des Signaux et Systèmes (L2S), CentraleSupélec-CNRS-Univ. Paris-Sud, Université Paris-Saclay, F91192, Gif-sur-Yvette, France (e-mail: {nolwenn.briquet-kerestedjian, maria.makarov, pedro.rodriguez}@centralesupelec.fr).*
[**] *CEA, LIST, Interactive Robotics Laboratory, F-91191 Gif-sur-Yvette, France (e-mail: {nolwenn.briquet, mathieu.grossard}@cea.fr).*

Abstract: This work proposes a design methodology for an observer-based impact detection with serial robot manipulators in presence of modeling uncertainties and using only proprioceptive sensors. After expressing modeling errors as the contribution of both dynamic parameters uncertainties and numerical differentiation errors, a Kalman filter is designed based on the inverse dynamic model with process and measurement power spectral densities explicitly depending on characterized uncertainties. The influence of the design parameters on the quality of the external torque estimation is studied in simulation and guidelines for tuning the Kalman filter are provided.

Keywords: Robotic manipulators, Fault detection, Observers, Kalman filters, Uncertainty, Parameter estimation.

1. INTRODUCTION

Whether for industrial or service applications, impact detection between a robot manipulator and its environment is of crucial importance, both to ensure the safety of the robot or the operator in case of unexpected collision and to ensure an efficient operation with fast switching from one operation to another for expected contacts with a fixture or part. When the safety of installation must be guaranteed at a high level, proprioceptive methods can be envisaged in addition with external sensing. Depending on the sensors installed in the robot manipulators, artificial skins, base/end-effector force sensors or joint torque sensors can provide information about the impact. In other cases, when only motor or joint position sensors are available as in Makarov et al. (2014), detection is still possible by exploiting the system dynamics by means of observers.

Quantitative model-based fault diagnostic methods developed in Venkatasubramanian et al. (2003); Ding (2008) offer a relevant framework for robot collision detection techniques without using any additional sensors since an impact can be related to a faulty behavior. In absence of redundant sensors, observer-based fault diagnosis presented in Frank and Ding (1997) are widely used to reconstruct measurements of the process with an observer using a quantitative mathematical model of the process. For instance, De Luca and Mattone (2004); Wahrburg et al. (2015a) propose a fault detection and isolation observer based on the generalized momentum for robot collision detection. However, these approaches rely on a model that can be affected by modeling errors. Then the external torque estimation reconstructs in the same structural way both the external disturbances and the modeling uncertainties, and no structural decoupling is reachable between both if the uncertainties are unstructured. Nevertheless, different frequency properties allow to discriminate collision from modeling uncertainties. This is why the previously proposed impact detection methods very often amount to some extent to bandpass filtering, either with fixed parameters in Jung et al. (2012) or with adaptive filters as in Makarov et al. (2014). In Wahrburg et al. (2015b), a Kalman filter for external force estimation is designed using the generalized momentum and considering friction model uncertainties to tune the filter parameters. Nonetheless, these approaches do not explicitly and systematically analyze the different uncertainties and estimation error sources, as well as their dependence on the robot trajectory, to characterize the filter parameters.

This work proposes an observer-based impact detection method for robot manipulators considering characterized uncertainties and provides high-level tuning guidelines. As previously in Briquet-Kerestedjian et al. (2016), uncertainties are expressed as a contribution of dynamic parameters and numerical differentiation errors, both determined for a given robot trajectory. A Kalman filter is derived based on the inverse dynamic model with process and measurement power spectral densities induced by the uncertainties characterization step. Finally, the influence of the design parameters on the detection is studied in simulation.

[1] This work was supported by grants from Digiteo France.

Notations	Description	Units (SI)
j	Unit imaginary number s.t. $j^2 = -1$	-
s	Laplace-domain variable	-
T_s	Sampling time	s
$\mathbf{0}_{i,k} \in \mathbb{R}^{i\times k}$	Matrix of zeros of dimension $i \times k$	-
$\boldsymbol{I}_i \in \mathbb{R}^{i\times i}$	Identity matrix of dimension i	-
$\boldsymbol{\chi} \in \mathbb{R}^{n_b}$	Rigid base parameters of the robot	-
$\boldsymbol{q} \in \mathbb{R}^n$	Joint angular position vector	rad
$\boldsymbol{M} \in \mathbb{R}^{n\times n}$	Robot inertia matrix	kg.m^2
$\boldsymbol{J}_m \in \mathbb{R}^{n\times n}$	Constant diagonal motor inertia matrix after reduction stage	kg.m^2
$\boldsymbol{M}_{rig} \in \mathbb{R}^{n\times n}$	Rigid robot inertia matrix with $\boldsymbol{M}_{rig}(\boldsymbol{q})=\boldsymbol{M}(\boldsymbol{q})+\boldsymbol{J}_m$	kg.m^2
$\boldsymbol{C}\dot{\boldsymbol{q}} \in \mathbb{R}^n$	Coriolis and centrifugal torques	Nm
$\boldsymbol{G} \in \mathbb{R}^n$	Gravity torque	Nm
$\boldsymbol{\tau}_f \in \mathbb{R}^n$	Friction torque	Nm
$\boldsymbol{\tau}_m \in \mathbb{R}^n$	Applied motor torque after reduction stage	Nm
$\boldsymbol{\tau}_{ext} \in \mathbb{R}^n$	External torque	Nm
$\boldsymbol{R}_{red} \in \mathbb{R}^{n\times n}$	Reduction matrix	-
$\boldsymbol{K}_{em} \in \mathbb{R}^{n\times n}$	Diagonal matrix of torque constants	Nm/A
$\boldsymbol{a}$	Any exact matrix or vector	-
$\boldsymbol{a}_\star$	Measured or estimated value of any exact matrix or vector $\boldsymbol{a}$	-
$\boldsymbol{\delta a}$	Error defined by $\boldsymbol{\delta a} = \boldsymbol{a}_\star - \boldsymbol{a}$	-
$\boldsymbol{a} \sim \mathcal{N}(\boldsymbol{\mu}, \boldsymbol{\sigma}^2)$	$\boldsymbol{a}$ follows a normal distribution with $\boldsymbol{\mu}$-mean and $\boldsymbol{\sigma}$-standard deviation	-

Table 1. Notations

After stating the problem in Section 2, a Kalman filter in presence of uncertainties is designed in Section 3. The influence of the Kalman settings is analyzed in simulation in Section 4. Section 5 draws a conclusion of this approach. Notations in Table 1 will be used throughout this study.

2. PROBLEM STATEMENT

This section briefly recalls the dynamic model of a rigid serial robot manipulator and reformulates it under a state-space form for further observer design. The uncertainties affecting these models are investigated.

2.1 Dynamic model and equivalent state-space representation

For a n-degrees of freedom (DOFs) rigid serial robot, its inverse dynamic model can be obtained from the Lagrangian formalism and is given by

$$\boldsymbol{M}_{rig}(\boldsymbol{q})\ddot{\boldsymbol{q}} + \boldsymbol{C}(\boldsymbol{q},\dot{\boldsymbol{q}})\dot{\boldsymbol{q}} + \boldsymbol{G}(\boldsymbol{q}) + \boldsymbol{\tau}_f = \boldsymbol{\tau}_m + \boldsymbol{\tau}_{ext} \quad (1)$$

In the following, without loss of generality and for the sake of simplicity only viscous friction will be considered but a more detailed friction model for collision detection can be found in Lee et al. (2015); Wahrburg et al. (2015b). The friction torque is expressed as $\boldsymbol{\tau}_f = \boldsymbol{F}_v\dot{\boldsymbol{q}}$ with $\boldsymbol{F}_v \in \mathbb{R}^n$ the diagonal matrix of viscous friction coefficients. For rigid robots with DC motors, the motor torque $\boldsymbol{\tau}_m$ can be obtained from the motor currents $\boldsymbol{i}_m$ by $\boldsymbol{\tau}_m = \boldsymbol{R}_{red}^T\boldsymbol{K}_{em}\boldsymbol{i}_m$. Robots with low friction levels and good backdrivable properties present a certain advantage for collision detection since any external torque will be precisely reflected on the motor currents without using any additional torque sensor (Makarov et al. (2014)).

By rewriting nonlinear terms in (1), a new input torque is calculated for impact monitoring as

$$\widetilde{\boldsymbol{\tau}} = \boldsymbol{\tau}_m - [\boldsymbol{M}(\boldsymbol{q})\ddot{\boldsymbol{q}} + \boldsymbol{C}(\boldsymbol{q},\dot{\boldsymbol{q}})\dot{\boldsymbol{q}} + \boldsymbol{G}(\boldsymbol{q})] \quad (2)$$

Note that (2) is a simple reformulation of the robot model and is completely independent from the actual robot feedback control. An equivalent dynamic model is thus obtained:

$$\boldsymbol{J}_m\ddot{\boldsymbol{q}} + \boldsymbol{F}_v\dot{\boldsymbol{q}} = \widetilde{\boldsymbol{\tau}} + \boldsymbol{\tau}_{ext} \quad (3)$$

which can be rewritten in an equivalent state-space form with $\boldsymbol{X} = \begin{bmatrix}\boldsymbol{q}^T & \dot{\boldsymbol{q}}^T\end{bmatrix}^T \in \mathbb{R}^{2n}$, $\boldsymbol{Y} = \boldsymbol{q} \in \mathbb{R}^n$ such as

$$\begin{cases}\dot{\boldsymbol{X}} = \boldsymbol{A}\boldsymbol{X} + \boldsymbol{B}\widetilde{\boldsymbol{\tau}} + \boldsymbol{B}\boldsymbol{\tau}_{\boldsymbol{ext}} \\ \boldsymbol{Y} = \boldsymbol{C}\boldsymbol{X}\end{cases} \quad (4)$$

where

$$\boldsymbol{A} = \begin{bmatrix}\mathbf{0}_{n,n} & \boldsymbol{I}_n \\ \mathbf{0}_{n,n} & -\boldsymbol{J}_m^{-1}\boldsymbol{F}_v\end{bmatrix};\ \boldsymbol{B} = \begin{bmatrix}\mathbf{0}_{n,n} \\ \boldsymbol{J}_m^{-1}\end{bmatrix};\ \boldsymbol{C} = [\,\boldsymbol{I}_n\ \mathbf{0}_{n,n}\,].$$

In this case, matrices $\boldsymbol{A}$, $\boldsymbol{B}$ and $\boldsymbol{C}$ are constant because $\boldsymbol{J}_m$ and $\boldsymbol{F}_v$ are constant but other models using time-varying matrices are also possible especially when dealing with Cartesian contact force estimation, which assumes that the location of the impact is known (see Wahrburg et al. (2015b)). The state-space representation (4) will further be used for observer design in Section 3.

2.2 Modeling uncertainties

The sources of uncertainties may be at least of two types: parametric uncertainties due to an imperfect knowledge of the robot parameters and coordinates errors due to measurement noise and numerical differentiation with respect to time (speed and acceleration estimations).

Parameters uncertainties For model-based approaches, robot dynamic parameters can be obtained from the nominal CAD data or identified experimentally as they can slightly differ from one robot to another or for different operating conditions. Their experimental identification described in Khalil and Dombre (2004) uses the fact that the inverse dynamic model (1) of an n-degrees of freedom rigid serial robot can be written as a linear regression with respect to the n_b rigid base parameters

$$\boldsymbol{\tau}_m = \boldsymbol{\varphi}(\boldsymbol{q},\dot{\boldsymbol{q}},\ddot{\boldsymbol{q}})\boldsymbol{\chi} \quad (5)$$

where $\boldsymbol{\varphi} \in \mathbb{R}^{n\times n_b}$ is the rigid regression matrix and $\boldsymbol{\chi} \in \mathbb{R}^{n_b}$ is the vector of rigid base parameters (i.e. the minimal set of identifiable parameters). For each link, the latter are obtained by linear combinations of the 6 components of the inertia tensor, the 3 components of the first moment and the mass, the total inertia moment for rotor actuator and gears, and the viscous friction coefficients.

After evaluating the identification model (5) at a sufficient number of points on several exciting trajectories, the vector $\boldsymbol{\chi}_\star$ of the identified base parameters can be obtained by least squares minimization of the 2-norm of the residual errors vector. Let $\boldsymbol{\delta\chi}$ be the vector of estimation errors:

$$\boldsymbol{\delta\chi} \overset{def}{=} \boldsymbol{\chi}_\star - \boldsymbol{\chi} \quad (6)$$

For the following, we assume that $\boldsymbol{\delta\chi}$ is Gaussian with zero-mean and standard deviation $\boldsymbol{\sigma}_{\boldsymbol{\chi}_\star}$ which can be obtained from the estimation of the standard deviation of the errors vector resulting from the identification. The

relative standard deviation $\%\boldsymbol{\sigma}_{\boldsymbol{\chi}_\star,i}$ of the i^{th} identified parameter is defined as

$$\%\boldsymbol{\sigma}_{\boldsymbol{\chi}_\star,i} = 100\frac{\boldsymbol{\sigma}_{\boldsymbol{\chi}_\star,i}}{|\boldsymbol{\chi}_{\star,i}|} \tag{7}$$

$\%\boldsymbol{\sigma}_{\boldsymbol{\chi}_\star,i}$ is used as a criterion to measure the quality of the identification of the i^{th} base parameter. In Khalil and Dombre (2004), the identification is considered acceptable if the relative standard deviation of a parameter is less than ten percent.

The resulting model errors are obtained by difference between the matrices evaluated with the identified parameters and with the exact parameters. For example for the robot inertia matrix,

$$\boldsymbol{\delta M}(\boldsymbol{q}) \overset{def}{=} \boldsymbol{M_\star}(\boldsymbol{q}) - \boldsymbol{M}(\boldsymbol{q}) \tag{8}$$

with $\boldsymbol{M_\star}$ and $\boldsymbol{M}$ denoting the robot inertia matrix evaluated respectively with the identified parameters and with the exact parameters. Calculating the difference between the inverse dynamic model evaluated with the identified and the exact parameters, an equivalent linear regression with respect to the estimation errors is obtained:

$$\boldsymbol{\delta M}_{rig}(\boldsymbol{q})\ddot{\boldsymbol{q}} + \boldsymbol{\delta C}(\boldsymbol{q},\dot{\boldsymbol{q}})\dot{\boldsymbol{q}} + \boldsymbol{\delta G}(\boldsymbol{q}) + \boldsymbol{\delta F}_v\dot{\boldsymbol{q}} = \boldsymbol{\varphi}(\boldsymbol{q},\dot{\boldsymbol{q}},\ddot{\boldsymbol{q}})\boldsymbol{\delta\chi} \tag{9}$$

Numerical differentiation errors Another origin of the errors comes from the numerical differentiation. Indeed, when only position sensors are integrated into the robot, in an industrial context velocities and accelerations are often rather approximated by finite differences from Taylor series than estimated by observers. We denote $\boldsymbol{q_\star}$ the measured joint positions and define $\dot{\boldsymbol{q}}_\star$ and $\ddot{\boldsymbol{q}}_\star$ respectively the joint velocities and accelerations obtained by numerical differentiation of $\boldsymbol{q_\star}$ with a numerical differentiation scheme of continuous filter D. We define $\boldsymbol{\delta\dot{q}}$ the vector of errors due to numerical differentiation of joint velocities as

$$\boldsymbol{\delta\dot{q}} \overset{def}{=} \dot{\boldsymbol{q}}_\star - \dot{\boldsymbol{q}} \tag{10}$$

Similarly we obtain $\boldsymbol{\delta\ddot{q}}$ for the joint accelerations.

Let $\boldsymbol{q_\star} = \boldsymbol{q} + \boldsymbol{\xi}$ be the noisy position measurement affected by a white bounded noise $\boldsymbol{\xi} \in \mathbb{R}^n$ due for instance to quantization. In the Laplace-domain, the error $\delta\dot{q}_i$ on the i^{th} axis velocity is given by

$$\Delta Q_d^i(s) = \underbrace{[D(s)-s]Q^i(s)}_{\text{approximated velocity-induced error}} + \underbrace{D(s)\xi^i(s)}_{\text{filtered noise}} \tag{11}$$

where $\Delta Q_d^i(s)$, $Q^i(s)$ and $\xi^i(s)$ are respectively the Laplace transforms of $\delta\dot{q}_i$, q_i and ξ_i for the i^{th} axis. Similarly we obtain the error $\delta\ddot{q}_i$ on the acceleration of axis i in the Laplace domain

$$\Delta Q_{dd}^i(s) = \left[D^2(s) - s^2\right] Q^i(s) + D^2(s)\xi^i(s) \tag{12}$$

with $\Delta Q_{dd}^i(s)$ the Laplace transform of $\delta\ddot{q}_i$ for the i^{th} axis.

The error with respect to the exact derivative of the signal is twofold: it contains an error term due to the derivative approximation, and an error term due to filtered measurement noise.

3. OBSERVER DESIGN FOR DETECTION UNDER UNCERTAINTIES

The impact of the uncertainties on the state-space representation (4) is first studied to then design a Kalman filter with noises of given power spectral densities (PSD).

3.1 State-space representation under uncertainties

In a more realistic approach, (2) is obtained using the estimated model parameters and the measured or calculated coordinates. Therefore it becomes

$$\widetilde{\boldsymbol{\tau}} = \boldsymbol{\tau}_m - [\boldsymbol{M_\star}(\boldsymbol{q_\star})\ddot{\boldsymbol{q}}_\star + \boldsymbol{C_\star}(\boldsymbol{q_\star},\dot{\boldsymbol{q}}_\star)\dot{\boldsymbol{q}}_\star + \boldsymbol{G_\star}(\boldsymbol{q_\star})] \tag{13}$$

The term (13) is in this case a compensation and may not be exact. This implies a compensation error $\boldsymbol{\delta\tau}_1$ such as

$$\begin{aligned}\boldsymbol{\delta\tau}_1 = {} & [\boldsymbol{M_\star}(\boldsymbol{q_\star})\ddot{\boldsymbol{q}}_\star + \boldsymbol{C_\star}(\boldsymbol{q_\star},\dot{\boldsymbol{q}}_\star)\dot{\boldsymbol{q}}_\star + \boldsymbol{G_\star}(\boldsymbol{q_\star})] \\ & - [\boldsymbol{M}(\boldsymbol{q})\ddot{\boldsymbol{q}} + \boldsymbol{C}(\boldsymbol{q},\dot{\boldsymbol{q}})\dot{\boldsymbol{q}} + \boldsymbol{G}(\boldsymbol{q})]\end{aligned} \tag{14}$$

The equivalent inverse dynamic model (3) becomes

$$\boldsymbol{J}_m\ddot{\boldsymbol{q}} + \boldsymbol{F}_v\dot{\boldsymbol{q}} = \widetilde{\boldsymbol{\tau}} + \boldsymbol{\tau}_{ext} + \boldsymbol{\delta\tau}_1 \tag{15}$$

With $\boldsymbol{J}_m = \boldsymbol{J}_{m\star} - \boldsymbol{\delta J}_m$ and $\boldsymbol{F}_v = \boldsymbol{F}_{v\star} - \boldsymbol{\delta F}_v$, it follows

$$\boldsymbol{J}_{m\star}\ddot{\boldsymbol{q}} + \boldsymbol{F}_{v\star}\dot{\boldsymbol{q}} = \widetilde{\boldsymbol{\tau}} + \boldsymbol{\tau}_{ext} + \underbrace{(\boldsymbol{\delta\tau}_1 + \boldsymbol{\delta J}_m\ddot{\boldsymbol{q}} + \boldsymbol{\delta F}_v\dot{\boldsymbol{q}})}_{\boldsymbol{\delta\tau}} \tag{16}$$

In the following, it is assumed that $\boldsymbol{M_\star}(\boldsymbol{q_\star}) \approx \boldsymbol{M_\star}(\boldsymbol{q})$, $\boldsymbol{C_\star}(\boldsymbol{q_\star},\dot{\boldsymbol{q}}_\star)\dot{\boldsymbol{q}} \approx \boldsymbol{C_\star}(\boldsymbol{q},\dot{\boldsymbol{q}})\dot{\boldsymbol{q}}$ and $\boldsymbol{G_\star}(\boldsymbol{q_\star}) \approx \boldsymbol{G_\star}(\boldsymbol{q})$ since small variations in $\boldsymbol{q}$ or $\dot{\boldsymbol{q}}$ induce small variations in the trigonometric or second-order functions of $\boldsymbol{M}_{rig\star}$, $\boldsymbol{C_\star}$ and $\boldsymbol{G_\star}$. Using (8) and (10) definitions, the global error term $\boldsymbol{\delta\tau}$ can then be rewritten as the sum of a contribution due to parameters uncertainties $\boldsymbol{\delta\tau^P} \in \mathbb{R}^n$ and of numerical differentiation errors $\boldsymbol{\delta\tau^D} \in \mathbb{R}^n$

$$\begin{aligned}\boldsymbol{\delta\tau^P} &= \boldsymbol{\delta M}_{rig}(\boldsymbol{q})\ddot{\boldsymbol{q}} + \boldsymbol{\delta C}(\boldsymbol{q},\dot{\boldsymbol{q}})\dot{\boldsymbol{q}} + \boldsymbol{\delta G}(\boldsymbol{q}) + \boldsymbol{\delta F}_v\dot{\boldsymbol{q}} \\ &= \boldsymbol{\varphi}(\boldsymbol{q},\dot{\boldsymbol{q}},\ddot{\boldsymbol{q}})\boldsymbol{\delta\chi}\end{aligned} \tag{17}$$

$$\boldsymbol{\delta\tau^D} = \boldsymbol{M_\star}(\boldsymbol{q_\star})\boldsymbol{\delta\ddot{q}} + \boldsymbol{C_\star}(\boldsymbol{q_\star},\dot{\boldsymbol{q}}_\star)\boldsymbol{\delta\dot{q}} \tag{18}$$

The state-space representation (4) in presence of uncertainties becomes

$$\begin{cases}\dot{\boldsymbol{X}} = \boldsymbol{A_\star X} + \boldsymbol{B_\star}(\widetilde{\boldsymbol{\tau}} + \boldsymbol{\delta\tau}) + \boldsymbol{B_\star\tau_{ext}} \\ \boldsymbol{Y_\star} = \boldsymbol{C_\star X} + \boldsymbol{\delta Y}\end{cases} \tag{19}$$

with $\boldsymbol{Y_\star} = \boldsymbol{q_\star}$, measurement noise $\boldsymbol{\delta Y} = \boldsymbol{\xi}$ and

$$\boldsymbol{A_\star} = \begin{bmatrix}\boldsymbol{0}_{n,n} & \boldsymbol{I}_n \\ \boldsymbol{0}_{n,n} & -\boldsymbol{J}_{m\star}^{-1}\boldsymbol{F}_{v\star}\end{bmatrix};\ \boldsymbol{B_\star} = \begin{bmatrix}\boldsymbol{0}_{n,n} \\ \boldsymbol{J}_{m\star}^{-1}\end{bmatrix};\ \boldsymbol{C_\star} = \begin{bmatrix}\boldsymbol{I}_n & \boldsymbol{0}_{n,n}\end{bmatrix}.$$

This representation in presence of uncertainties will be used in the next section for the design of a Kalman filter.

3.2 Kalman filter design

For the purpose of collision detection and reconstruction, a disturbance observer with the augmented state $\boldsymbol{X}_{aug} = [\boldsymbol{X}^T \quad \boldsymbol{\tau_{ext}}^T]^T$ is studied. The external torque is modeled by a first-order model such as

$$\dot{\boldsymbol{\tau}}_{ext} = \boldsymbol{A}_{ext}\boldsymbol{\tau}_{ext} - \boldsymbol{A}_{ext}\boldsymbol{w}_{ext}\,, \tag{20}$$

where $\boldsymbol{A}_{ext} \in \mathbb{R}^{n\times n}$ is a diagonal matrix of strictly negative terms that accounts for the dynamics of the collision, and $\boldsymbol{w}_{ext} \in \mathbb{R}^n \sim \mathcal{N}(0, \boldsymbol{W}_{ext})$ is a white noise reflecting the uncertainties on the disturbance model (20).

Therefore, the following augmented state-space model is used for the design of the Kalman filter

$$\begin{cases}\dot{\boldsymbol{X}}_{aug} = \boldsymbol{A}_{aug}\boldsymbol{X}_{aug} + \boldsymbol{B}_{aug}\widetilde{\boldsymbol{\tau}} + \boldsymbol{F}\boldsymbol{w} \\ \boldsymbol{Y_\star} = \boldsymbol{C}_{aug}\boldsymbol{X}_{aug} + \boldsymbol{v}\end{cases} \tag{21}$$

with

$$\boldsymbol{A}_{aug} = \begin{bmatrix}\boldsymbol{A_\star} & \boldsymbol{B_\star} \\ \boldsymbol{0}_{n,2n} & \boldsymbol{A}_{ext}\end{bmatrix};\ \boldsymbol{B}_{aug} = \begin{bmatrix}\boldsymbol{B_\star} \\ \boldsymbol{0}_{n,n}\end{bmatrix};$$

$$\boldsymbol{F} = \begin{bmatrix}\boldsymbol{B_\star} & \boldsymbol{0}_{2n,n} \\ \boldsymbol{0}_{n,n} & -\boldsymbol{A}_{ext}\end{bmatrix};\ \boldsymbol{C}_{aug} = \begin{bmatrix}\boldsymbol{C_\star} & \boldsymbol{0}_{n,n}\end{bmatrix}.$$

where $\boldsymbol{w} = \begin{bmatrix}\boldsymbol{\delta\tau}^T & \boldsymbol{w}_{ext}{}^T\end{bmatrix}^T \in \mathbb{R}^{2n}$ and $\boldsymbol{v} = \boldsymbol{\xi} \in \mathbb{R}^n$ are respectively process and measurement noises, assumed

to be independent centered Gaussian white noises of PSD respectively $\boldsymbol{W}$ and $\boldsymbol{V}$. Matrices $\boldsymbol{A}_{aug}$, $\boldsymbol{B}_{aug}$, $\boldsymbol{C}_{aug}$, $\boldsymbol{F}$, $\boldsymbol{W}$, $\boldsymbol{V}$ are then discretized for the Kalman synthesis:

$$\boldsymbol{A}^d_{aug} = e^{\boldsymbol{A}_{aug}T_s}\ ;\ \boldsymbol{B}^d_{aug} = \int_0^{T_s} e^{\boldsymbol{A}_{aug}\nu}\boldsymbol{B}_{aug}\,\mathrm{d}\nu\ ;\ \boldsymbol{C}^d_{aug} = \boldsymbol{C}_{aug}\ ;$$
$$\boldsymbol{F}^d = \boldsymbol{I}_n\ ;\quad \boldsymbol{W}^d \approx T_s\,\boldsymbol{F}\,\boldsymbol{W}\,\boldsymbol{F}^T\ ;\ \boldsymbol{V}^d = \boldsymbol{V}\,/\,T_s\,. \tag{22}$$

where $\square^d$ holds for discrete-time model matrices. Based on (21) and (22), a discrete Kalman filter is designed and the estimated state is given by

$$\begin{cases} \hat{\boldsymbol{X}}_{aug}(k+1) = \boldsymbol{A}^d_{aug}\hat{\boldsymbol{X}}_{aug}(k) + \boldsymbol{B}^d_{aug}\widetilde{\boldsymbol{\tau}}(k) \\ \qquad +\boldsymbol{K}_f\left[\boldsymbol{Y}(k+1) - \boldsymbol{C}^d_{aug}\left(\boldsymbol{A}^d_{aug}\hat{\boldsymbol{X}}_{aug}(k) + \boldsymbol{B}^d_{aug}\widetilde{\boldsymbol{\tau}}(k)\right)\right] \\ \hat{\boldsymbol{Y}}(k) = \boldsymbol{C}^d{}_{aug}\hat{\boldsymbol{X}}_{aug}(k) \end{cases} \tag{23}$$

where $\boldsymbol{K}_f$ is the asymptotic Kalman gain computed at each time step for given $\boldsymbol{W}^d$ and $\boldsymbol{V}^d$ (see Section 3.3).

3.3 Uncertainties-induced power spectral densities

In Section 2.2, it has been assumed that $\boldsymbol{\delta\chi} \sim \mathcal{N}(0, \boldsymbol{\sigma}^2_{\boldsymbol{\chi}_\star})$ with $\boldsymbol{\sigma}^2_{\boldsymbol{\chi}_\star} \in \mathbb{R}^{n_b \times n_b}$ the diagonal covariance matrix of $\boldsymbol{\chi}_\star$. Given (17), by linearity $\boldsymbol{\delta\tau^P}$ is also Gaussian such that $\boldsymbol{\delta\tau^P} \sim \mathcal{N}(0, \boldsymbol{\varphi}\,\boldsymbol{\sigma}^2_{\boldsymbol{\chi}\star}\,\boldsymbol{\varphi}^T)$ where the arguments have been omitted for the sake of brevity. Therefore $\boldsymbol{\delta\tau^P}$ is approximated by a white noise of PSD

$$\boldsymbol{W}_{\delta\tau^P} = \boldsymbol{\varphi}_{ref}\,\boldsymbol{\sigma}^2_{\boldsymbol{\chi}\star}\,\boldsymbol{\varphi}^T_{ref} \tag{24}$$

where $\boldsymbol{\varphi}_{ref} = \boldsymbol{\varphi}(\boldsymbol{q}_{ref}, \dot{\boldsymbol{q}}_{ref}, \ddot{\boldsymbol{q}}_{ref})$ is evaluated on the reference trajectory.

According to (11) and (12), the numerical differentiation errors $\boldsymbol{\delta\dot{q}}$ and $\boldsymbol{\delta\ddot{q}}$ result from contributions of derivation approximation-induced errors and sensor noise. Both terms are approximated by a white noise, thus by linearity $\boldsymbol{\delta\tau^D}$ is also approximated by a white noise of PSD $\boldsymbol{W}_{\delta\tau^D}$ calculated on the reference trajectory in a similar way as for $\boldsymbol{W}_{\delta\tau^P}$ (see Appendix A for details).

Consequently, the uncertainties-induced PSD is defined by $\boldsymbol{W}_{\delta\tau} = \boldsymbol{W}_{\delta\tau^P} + \boldsymbol{W}_{\delta\tau^D}$. Finally the global PSD for process noise will be

$$\boldsymbol{W} = \begin{bmatrix} \boldsymbol{W}_{\delta\tau} & \boldsymbol{0}_{n,n} \\ \boldsymbol{0}_{n,n} & \boldsymbol{W}_{ext} \end{bmatrix} \tag{25}$$

The measurement noise $\boldsymbol{v}$ is assumed to be a white Gaussian noise due to quantization. Its PSD is given by

$$[V]_{ik} = \begin{cases} \frac{r_i^2}{12} & \text{if } i = k \\ 0 & \text{else} \end{cases} \tag{26}$$

with r_i the joint encoder resolution for axis i.

4. GUIDELINES FOR OBSERVER TUNING

The influence of the Kalman filter design parameters on the estimation $\hat{\boldsymbol{\tau}}_{\boldsymbol{ext}}$ of the external torque is studied in simulation in the rigid case. The case study concerns a 6-DOF robot manipulator presented in Fig. 1, where joint positions are available from position sensors on each joint.

For the simulations, each axis is controlled in position with a Proportional-Integral-Derivative (PID) control law. The sampling time is 1 ms. The configurations tested in simulation are combinations of $[U_i, W_j, A_k]$ for a fixed trajectory type T and differentiation method D (see Table 2).

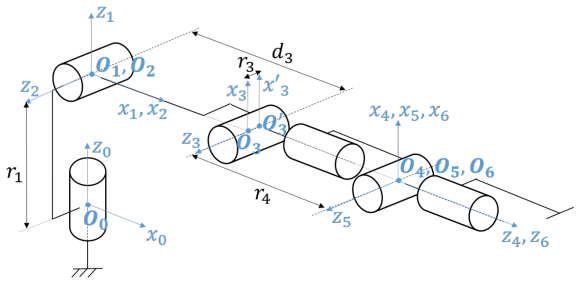

Fig. 1. Kinematic chain of serial robot manipulator and associated frames in the modified Denavit-Hartenberg convention from Khalil and Dombre (2004)

Trajectory	T : Sinusoidal for the 6 axes $E_0 = [0.2, 0.2, 0.2, 0.2, 0.2, 0.2]$ rad $f_0 = [0.7, 0.6, 0.5, 0.4, 0.3, 0.2]$ Hz
$\%\boldsymbol{\sigma}_{\boldsymbol{\chi}_\star,i}$, $i = 1..n_b$	$U_1 : [-5\%, 5\%]$ $U_2 : [-20\%, 20\%]$
Numerical differentiation scheme	D : First-order low-pass filtered derivative of cut-off frequency $\omega_c = 2\pi 40$ rad/s $\sigma^2_{d_j} = 5.61 \cdot 10^4\,\sigma^2_{\xi_j}$; $\sigma^2_{dd_j} = 3.35 \cdot 10^9\,\sigma^2_{\xi_j}$
$\boldsymbol{W}_{ext}$	$W_1 : diag([20; 15; 30; 0.1; 0.02; 0.01])$ $W_2 : 10^4 diag([20; 15; 30; 0.1; 0.02; 0.01])$
$\boldsymbol{A}_{ext}$	$A_1 : -0.1\boldsymbol{I}_n$ $A_2 : -\boldsymbol{I}_n$ $A_3 : -10\boldsymbol{I}_n$

Table 2. Simulated configurations

In particular, we will study the influence of :

- Parameters uncertainties through the relative standard deviation $\%\boldsymbol{\sigma}_{\boldsymbol{\chi}_\star}$ of each identified parameter. Thus the covariance matrix $\boldsymbol{\sigma}^2_{\boldsymbol{\chi}_\star}$ of the estimated parameters is used to calculate $\boldsymbol{W}_{\delta\tau^P}$;
- The external torque model (20) through the matrix $\boldsymbol{A}_{ext}$ and the PSD $\boldsymbol{W}_{ext}$.

We could also study the influence of the numerical differentiation scheme D through the PSD $\boldsymbol{W}_{\delta\tau^D}$, and the reference trajectory T that affects both $\boldsymbol{W}_{\delta\tau^P}$ and $\boldsymbol{W}_{\delta\tau^D}$, but for the sake of clarity we limit this study to these 3 varying cases. All of these design parameters affect the asymptotic Kalman gain and thus the estimation $\hat{\boldsymbol{\tau}}_{ext}$. Their effect on $\hat{\boldsymbol{\tau}}_{ext}$ is studied in presence of an external torque $\boldsymbol{\tau}_{ext} = [20, 40, 15, 1, 1, 1]$Nm applied on one axis after the other in order to emphasize the effects on each axis. Fig. 2 illustrates the results for axis 2.

To obtain a good reconstruction of the external disturbance, $\hat{\boldsymbol{\tau}}_{ext}$ must have a minimum rise time and a static error as low as possible. From Fig. 2, we see that the greater the PSD of the uncertainties is, the greater the static error is. Moreover, the greater $\boldsymbol{A}_{ext}$ and $\boldsymbol{W}_{ext}$ are, the smaller the time response and the static error are, but the less filtered the uncertainties are. Finally, for tuning the filter for the external torque estimation in collision detection, a trade-off between good estimation and sufficient filtering of uncertainties is to be found. On the basis of these criteria, the Kalman filter has to be tuned with significant $\boldsymbol{A}_{ext}$ and $\boldsymbol{W}_{ext}$, while attempting to minimize parameters uncertainties during the identification step to reduce their contribution.

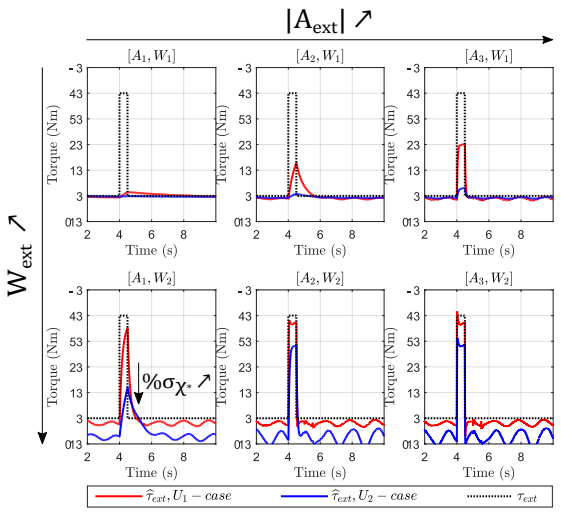

Fig. 2. External torque estimates for several $[T, U_i, D, W_j, A_k]$-configurations for axis 2

5. CONCLUSION

In this paper, a Kalman filter for robot collision detection is designed in presence of characterized uncertainties. The uncertainties-induced errors have been decomposed into a combination of parameters estimation and numerical differentiation errors and this characterization is used to tune a Kalman filter in order to estimate the external torque. The influence of the design parameters on the detection has been studied through simulation results.

A frequency analysis can complete this approach to determine the impact of the frequency characteristics of the Kalman filter on the estimation of the external torque. The same methodology could be applied to other model-based methods, such as general momentum-based methods, in order to compare their performance in presence of uncertainties and determine the favorable cases for each method. Finally, a future study could be conducted focusing on determining the spatial positioning, amplitude and direction of the collision by considering the Cartesian-space level model.

Appendix A. CALCULATION OF $\boldsymbol{W}_{\delta\tau^D}$

As detailed in Briquet-Kerestedjian et al. (2016), for a given position trajectory characterized by velocities and accelerations respectively bounded by $\boldsymbol{v_{max}}$ and $\boldsymbol{a_{max}}$, the first term of (11) and (12) which are due to derivative approximation can respectively be bounded by

$$A^i_{\dot{q}} = |D(j\omega^i_{eq}) - j\omega^i_{eq}|E^i_{eq} \tag{A.1}$$

$$A^i_{\ddot{q}} = |D(j\omega^i_{eq})^2 - (j\omega^i_{eq})^2|E^i_{eq} \tag{A.2}$$

where $E^i_{eq} = (v^i_{max})^2/a^i_{max}$ and pulsation $\omega^i_{eq} = a^i_{max}/v^i_{max}$.

For the filtered noise term, if the input noise ξ_i is white of variance $\sigma^2_{\xi_i}$ in the discrete-time domain (e.g. quantization noise), the output noise filtered by the equivalent discrete-time filter $\bar{D}(z)$ (of impulse response $d[k]$) is Gaussian of variance $\sigma^2_{\dot{q}_i} = \sigma^2_{\xi_i} \sum_{k=-\infty}^{\infty} d^2[k]$, and similarly for $\sigma^2_{\ddot{q}_i}$.

Finally, $\boldsymbol{\delta\dot{q}}$ and $\boldsymbol{\delta\ddot{q}}$ can be bounded at 99,7% respectively by $\pm(\boldsymbol{A}_{\dot{q}} + 3\boldsymbol{\sigma}_{\dot{q}})$ and $\pm(\boldsymbol{A}_{\ddot{q}} + 3\boldsymbol{\sigma}_{\ddot{q}})$. Then $\boldsymbol{\delta\dot{q}}$ and $\boldsymbol{\delta\ddot{q}}$ are approximated by equivalent noises of respective PSD $\boldsymbol{\sigma}^2_{\delta\dot{q}}$ and $\boldsymbol{\sigma}^2_{\delta\ddot{q}}$ such as

$$\boldsymbol{\sigma}^2_{\delta\dot{q}} = \left(\frac{1}{3}\boldsymbol{A}_{\dot{\boldsymbol{q}}} + \boldsymbol{\sigma}_{\dot{\boldsymbol{q}}}\right)^2 \quad ; \quad \boldsymbol{\sigma}^2_{\delta\ddot{q}} = \left(\frac{1}{3}\boldsymbol{A}_{\ddot{\boldsymbol{q}}} + \boldsymbol{\sigma}_{\ddot{\boldsymbol{q}}}\right)^2 \tag{A.3}$$

where for each term the two contributions are assumed to be independent. Thus by linearity, the PSD of $\boldsymbol{\delta\tau}^D$ detailed in (18) is deduced with the matrices $\boldsymbol{M}$ and $\boldsymbol{C}$ evaluated along the reference trajectory such as:

$$\begin{aligned}\boldsymbol{W}_{\delta\tau^D}(t) = {} & \boldsymbol{M}_\star(\boldsymbol{q_{ref}})\, \boldsymbol{\sigma}^2_{\delta\ddot{q}}\, \boldsymbol{M}_\star(\boldsymbol{q_{ref}})^T \\ & + \boldsymbol{C}_\star(\boldsymbol{q_{ref}}, \dot{\boldsymbol{q}}_{\boldsymbol{ref}})\, \boldsymbol{\sigma}^2_{\delta\dot{q}}\, \boldsymbol{C}_\star(\boldsymbol{q_{ref}}, \dot{\boldsymbol{q}}_{\boldsymbol{ref}})^T\end{aligned} \tag{A.4}$$

where $\boldsymbol{\delta\dot{q}}$ and $\boldsymbol{\delta\ddot{q}}$ are assumed to be independent noises.

REFERENCES

Briquet-Kerestedjian, N., Makarov, M., Grossard, M., and Rodriguez-Ayerbe, P. (2016). Quantifying the uncertainties-induced errors in robot impact detection methods. In *IECON 2016 - 42nd Annual Conference of the IEEE Industrial Electronics Society*, 5328–5334. doi:10.1109/IECON.2016.7793186.

De Luca, A. and Mattone, R. (2004). An adapt-and-detect actuator FDI scheme for robot manipulators. In *IEEE International Conference on Robotics and Automation (ICRA), 2004*, volume 5, 4975–4980.

Ding, S. (2008). *Model-based fault diagnosis techniques: design schemes, algorithms, and tools*. Springer Science & Business Media.

Frank, P.M. and Ding, X. (1997). Survey of robust residual generation and evaluation methods in observer-based fault detection systems. *Journal of process control*, 7(6), 403–424.

Jung, B.J., Choi, H.R., Koo, J.C., and Moon, H. (2012). Collision detection using band designed disturbance observer. In *IEEE International Conference on Automation Science and Engineering (CASE), 2012*, 1080–1085. doi:10.1109/CoASE.2012.6386389.

Khalil, W. and Dombre, E. (2004). *Modeling, identification and control of robots*. Butterworth-Heinemann.

Lee, S.D., Kim, M.C., and Song, J.B. (2015). Sensorless collision detection for safe human-robot collaboration. In *IEEE/RSJ International Conference on Intelligent Robots and Systems (IROS), 2015*, 2392–2397. doi: 10.1109/IROS.2015.7353701.

Makarov, M., Caldas, A., Grossard, M., Rodriguez-Ayerbe, P., and Dumur, D. (2014). Adaptive filtering for robust proprioceptive robot impact detection under model uncertainties. *IEEE/ASME Transaction on Mechatronics*, 19(6), 1917–1928. doi: 10.1109/TMECH.2014.2315440.

Venkatasubramanian, V., Rengaswamy, R., Yin, K., and Kavuri, S.N. (2003). A review of process fault detection and diagnosis: Part I: Quantitative model-based methods. *Computers & chemical engineering*, 27(3), 293–311.

Wahrburg, A., Matthias, B., and Ding, H. (2015a). Cartesian contact force estimation for robotic manipulators-a fault isolation perspective. *IFAC-PapersOnLine*, 48(21), 1232–1237.

Wahrburg, A., Morara, E., Cesari, G., Matthias, B., and Ding, H. (2015b). Cartesian contact force estimation for robotic manipulators using kalman filters and the generalized momentum. In *IEEE International Conference on Automation Science and Engineering (CASE), 2015*, 1230–1235. doi:10.1109/CASE.2015.7294266.